Canadian Science Publishing | Transactions of the Canadian Society for Mechanical Engineering

# Study on a 4-DOF multi-dimensional vibration isolation platform based on 4-UPU parallel mechanism



| | |
|---|---|
| Journal: | *Transactions of the Canadian Society for Mechanical Engineering* |
| Manuscript ID | TCSME-2020-0142.R2 |
| Manuscript Type: | Article |
| Date Submitted by the Author: | 18-Jan-2021 |
| Complete List of Authors: | Zhang, Ying; Beijing Jiaotong University, Depatment of Mechanical Engineering in School of Mechanical, Electronic and Control Engineering<br>Guo, Xiaodong; Beijing Jiaotong University, School of Mechanical, Electronic and Control Engineering<br>Yu, Shijia; Beijing Jiaotong University |
| Keywords: | Multi-dimensional vibration, vibration isolation, 4-UPU parallel mechanism, vibration response analysis, vibration model |
| Is the invited manuscript for consideration in a Special Issue? : | Not applicable (regular submission) |
| | |

# Study on a 4-DOF multi-dimensional vibration isolation platform based on 4-UPU parallel mechanism

Ying Zhang [1*], Xiaodong Guo[1], Shijia Yu[1]

[1]*School of Mechanical, Electronic and Control Engineering, Beijing Jiaotong University, Beijing, China*

*E-mail: yzhang2@bjtu.edu.cn*

*Corresponding author

**Abstract:** A novel 4-DOF (degrees of freedom) multi-dimensional vibration isolation platform (MDVIP) based on 4-UPU (U denotes universal joint, P denotes prismatic joint) parallel mechanism is put forward for vibration isolation of the sensitive devices. It consists of 4 limbs and each limb has two universal joints and a module of spring damper. The kinematic model and vibration model of the proposed MDVIP are established and analyzed. The main dimensions of the MDVIP and the parameters of the spring damper module are designed by optimization method to meet various design requirements and constraints. Both the virtual prototype and physical prototype of the MDVIP are built to testify the vibration isolation performance. The results of numerical calculation, simulation and experimental studies based on vibration response analysis show that the proposed MDVIP can isolate at least 78% vibration from the fixed base in three axial directions and 64% vibration in the direction around the *Z*-axis, and thus may attenuate the disturbances to the items on the moving platform to a large extent.



**Keywords:** Multi-dimensional vibration; vibration isolation; 4-UPU parallel mechanism; vibration response analysis; vibration model

## 1 Introduction

Multi-dimensional vibration isolation platforms (MDVIP) are widely used in dynamic environments for their high adaptability to different circumstances. Compared with the single-dimensional isolator, MDVIP can not only isolate the vibration from one or more dimensions but also adjust its position quickly to keep the devices in a steady state. Compared with the normal MDVIPs, the one based on a parallel mechanism has better performance in carrying capacity and dynamic stability, which makes it a promising solution for multi-dimensional vibration isolation.

The first parallel mechanism used for vibration isolation was Stewart platform (Geng 1994). To investigate the influence of structural parameters on the vibration isolation performance of Stewart platform, the motion and dynamic models of Stewart platform under impulsive disturbance were built based on Newton-Euler method, Virtual Work Principle and Kane's method (Selig 2001; Liu 2006; Yi 2014; Wu 2015). Thayer (2002) studied the influence of end flexure rotational stiffness on Stewart platform. Hauge (2004) explored the influence of wire harness on the vibration isolation of Stewart platform. Wu (2017) optimized the payload and strut mass of Stewart platform. To improve the vibration isolation performance, quasi-zero-stiffness isolators, multi-directional elasticity isolators, and adjustable stiffness isolators were developed (Zhou 2017; Qin 2020; Wang 2020). Also, hybrid isolation platforms with passive and active components were presented to realize whole frequency vibration isolation(Lee 2016; Chi 2020). Fan (2018) studied the integrated dynamic modeling for a Stewart platform. Yang (2019; 2020) proposed an isotropic control framework for the flexible Stewart platform and verified its vibration isolation capabilities by simulation and experiments.

In the situations that the devices are not subject to full directional vibration, lower-mobility parallel mechanisms were introduced. Type synthesis, kinematics, and singular configuration of the lower-mobility parallel mechanism were fully studied (Wei 2019; Ye 2018; Liu 2018; Pan 2017). Sun (2010) divided the workspace of a 4-DOF parallel mechanism into position-orientation coupling (POC) subspace and one position-feed (PF) subspace and optimized the hybrid module in a global view. Song(2014a; 2014b) optimized the force and motion transmissibility of a 1T3R parallel mechanism by genetic algorithm and optimized the kinematic performance index of a 5-DOF parallel mechanism by nondominated sorting genetic algorithm II. Lian (2015) built the stiffness model considering the gravitational effects of a 5-DOF parallel mechanism and obtained the stiffness values by experiment. Sun (2018; 2019) built the elastodynamic model of a 5-DOF parallel kinematic machine(PKM) with considering geometric errors and developed an optimization method with taking parameter uncertainty into account to make the prototype of PKM have minimal vibration and deformation.

The vibration isolation platforms based on lower-mobility parallel mechanisms are more suitable for the low-dimensional vibration situation where the degrees of freedom (DOFs) of the mechanisms are consistent with the vibration directions. Temmerman (2004; 2005) built a 4-RPR platform to isolate the vibration exerted on agricultural machinery drivers. Yang (2013) designed a 3-DOF MDVIP based on a 3-PRC parallel mechanism to reduce the vibration of stretchers during vehicles moving. Guo (2014) proposed a kind of 4-CPS/RPS parallel mechanism for shipboard active vibration isolation. Wang (2017) presented a vibration isolation platform based on 3-UPU/UPU parallel mechanism with flexure hinges for whole-spacecraft vibration isolation.

The moving vehicles will be subjected to horizontal vibration during acceleration and deceleration, angular vibration during turning, and vertical vibration on the bumpy road. The devices in moving vehicles will suffer the vibrations in lateral, longitudinal, vertical, and torsional directions. For the vibration-sensitive devices, the accuracy and service life will be deteriorated due to the vibrations. To reduce the impact of vibration on them, the vibration isolation platform should have appropriate DOF in three translation directions and one rotation direction. A 4-DOF parallel mechanism with the above-mentioned mobility can meet the requirement of the MDVIP. Considering the stability of the vibration isolation platform, the limbs of the 4-DOF parallel mechanism should be the same. Furthermore, to make the parallel mechanism suitable for converting to a vibration isolation platform, the limb should include at least a prismatic joint which can be easily replaced by the spring damping module. As a result, the 4-UPU parallel mechanism is selected as the basic mechanism for the vehicle vibration isolation platform. In this paper, the dimension parameters of 4-UPU will be optimized for better carrying capacity and motion stability. The vibration model will be built based on Virtual Work Principle. For better isolation performance, the stiffness and damping of each limb will be optimized by Genetic Algorithm. And the isolation effects of the proposed MDVIP will be verified by theoretical analysis, simulation and experiments.

## 2 Kinematics analysis and optimization of the 4-UPU mechanism

### 2.1 Kinematics analysis

4-UPU parallel mechanism shown in Fig.1 is a kind of 4-DOF mechanism with a relatively simple configuration, which consists of four identical kinematic limbs and each limb has two universal (U) joints and one prismatic (P) joint. According to screw theory, when axes 1 of the two U joints of a limb are perpendicular to the upper and the lower platform respectively, and axes 2 of the two U joints are parallel to each other, the 4-UPU parallel mechanism will provide four DOFs, including translation along $x$-, $y$- and $z$-axis and rotation about the $z$-axis.

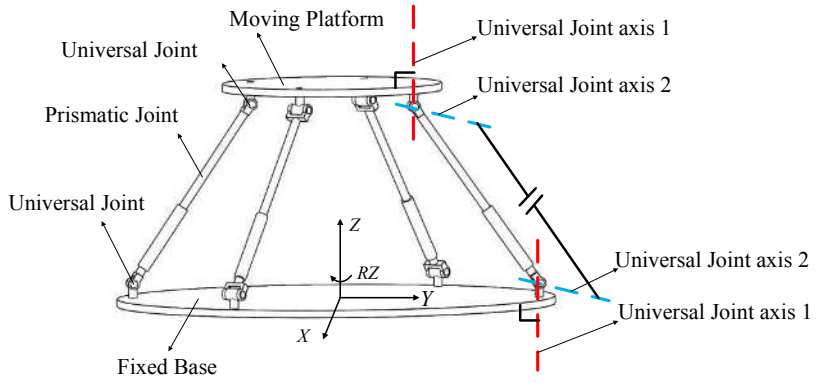


Fig. 1 Mechanism of 4-UPU

As shown in Fig.2, the coordinate-system *O-XYZ* is set at the geometric center of fixed base *O* and the coordinate-system *o-xyz* is set at the geometric center of moving platform *o*. The coordinates of the connection points $a_1$, $a_2$, $a_3$, $a_4$ in *O-XYZ* and $b_1$, $b_2$, $b_3$, $b_4$ in *o-xyz* can be expressed as:

$$\begin{cases} a_1^O=(X_{a1} \quad Y_{a1} \quad Z_{a1})=(-R_1 \quad R_2 \quad 0) \\ a_2^O=(X_{a2} \quad Y_{a2} \quad Z_{a2})=(-R_1 \quad -R_2 \quad 0) \\ a_3^O=(X_{a3} \quad Y_{a3} \quad Z_{a4})=(R_1 \quad -R_2 \quad 0) \\ a_4^O=(X_{a4} \quad Y_{a4} \quad Z_{a4})=(R_1 \quad R_2 \quad 0) \end{cases} \quad \begin{cases} b_1^o=(x_{b1} \quad y_{b1} \quad z_{b1})=(-d \quad d \quad 0) \\ b_2^o=(x_{b2} \quad y_{b2} \quad z_{b2})=(-d \quad -d \quad 0) \\ b_3^o=(x_{b3} \quad y_{b3} \quad z_{b3})=(d \quad -d \quad 0) \\ b_4^o=(x_{b4} \quad y_{b4} \quad z_{b4})=(d \quad d \quad 0) \end{cases} \tag{1}$$

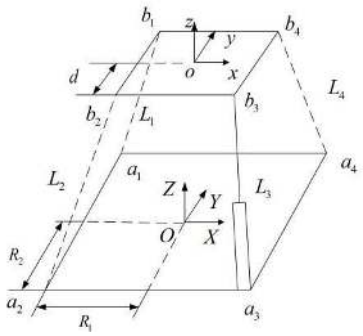


Fig. 2 The Cartesian coordinate system of the 4-UPU mechanism

To build the relationship between the limbs and the moving platform, the connection points $b_i$ ($i$=1,2,3,4) in *o-xyz* need to be transformed into the ones in *O-XYZ*. According to the theory of coordinate transformation, the coordinate of $b_i^o$ in *O-XYZ* can be expressed by the position coordinate of *o-xyz* in *O-XYZ*, which is defined as [$X_o$, $Y_o$, $Z_o$, $\gamma$]. Therefore, the transform matrix of *o-xyz* can be expressed as:

$$\mathbf{T}_\mathbf{o}^\mathbf{O}=\begin{bmatrix} \cos\gamma & -\sin\gamma & 0 & X_o \\ \sin\gamma & \cos\gamma & 0 & Y_o \\ 0 & 0 & 1 & Z_o \\ 0 & 0 & 0 & 1 \end{bmatrix} \tag{2}$$

And the coordinate of $b_i^o$ in *O-XYZ* can be expressed as:

$$b_i^O = \mathbf{T}_\mathbf{o}^\mathbf{O} b_i^o \tag{3}$$

By transferring the connection points of the 4-UPU parallel mechanism into *O-XYZ*, the motion constraint equations of 4-UPU can be expressed as:

$$L_i^2 = b_i^O - a_i^O = (X_{bi} - X_{ai})^2 + (Y_{bi} - Y_{ai})^2 + (Z_{bi} - Z_{ai})^2 \quad (i = 1,2,3,4) \tag{4}$$

where $L_i$ ($i$=1,2,3,4) is the length of the $i$th limb.

Based on the position coordinate [$X_o$, $Y_o$, $Z_o$, $\gamma$] of *o-xyz* in *O-XYZ*, the motion constraint equations are transferred into:

$$\begin{aligned}
&L_1^2 - (-d\sin\gamma - d\cos\gamma + X_o + R_1)^2 - (-d\sin\gamma + d\cos\gamma + Y_o - R_2)^2 - Z_o^2 = 0\\
&L_2^2 - (d\sin\gamma - d\cos\gamma + X_o + R_1)^2 - (-d\sin\gamma - d\cos\gamma + Y_o + R_2)^2 - Z_o^2 = 0\\
&L_3^2 - (d\sin\gamma + d\cos\gamma + X_o - R_1)^2 - (d\sin\gamma - d\cos\gamma + Y_o + R_2)^2 - Z_o^2 = 0\\
&L_4^2 - (-d\sin\gamma + d\cos\gamma + X_o - R_1)^2 - (d\sin\gamma + d\cos\gamma + Y_o - R_2)^2 - Z_o^2 = 0
\end{aligned} \tag{5}$$

And then, the Jacobi matrix is calculated through the differential equations of motion constraints:

$$\mathbf{J}^{-1} = \begin{bmatrix}
\dfrac{-ds\gamma - dc\gamma + X_o + R_1}{L_1} & \dfrac{-ds\gamma + dc\gamma + Y_o - R_2}{L_1} & \dfrac{Z_o}{L_1} & \dfrac{D_1}{L_1}d\\
\dfrac{ds\gamma - dc\gamma + X_o + R_1}{L_2} & \dfrac{-ds\gamma - dc\gamma + Y_o + R_2}{L_2} & \dfrac{Z_o}{L_2} & \dfrac{D_2}{L_2}d\\
\dfrac{ds\gamma + dc\gamma + X_o - R_1}{L_3} & \dfrac{ds\gamma - dc\gamma + Y_o + R_2}{L_3} & \dfrac{Z_o}{L_3} & \dfrac{D_3}{L_3}d\\
\dfrac{-ds\gamma + dc\gamma + X_o - R_1}{L_4} & \dfrac{ds\gamma + dc\gamma + Y_o - R_2}{L_4} & \dfrac{Z_o}{L_4} & \dfrac{D_4}{L_4}d
\end{bmatrix} \tag{6}$$

where,

$$\begin{aligned}
D_1 &= (X_o + R_1)(\sin\gamma - \cos\gamma) + (-Y_o + R_2)(\sin\gamma + \cos\gamma)\\
D_2 &= (X_o + R_1)(\sin\gamma + \cos\gamma) + (Y_o + R_2)(\sin\gamma - \cos\gamma)\\
D_3 &= (-X_o + R_1)(\sin\gamma - \cos\gamma) + (Y_o + R_2)(\sin\gamma + \cos\gamma)\\
D_4 &= (-X_o + R_1)(\sin\gamma + \cos\gamma) + (-Y_o + R_2)(\sin\gamma - \cos\gamma)
\end{aligned} \tag{7}$$

Based on the equations above, the relationship between the limbs and the positions of the moving platform has been built. And the parameters of the 4-UPU parallel mechanism will be optimized for better performance.

**2.2 Optimal design of the dimension parameters**

The workspace, carrying capacity, and motion stability of the parallel mechanism are taken as the considered performance indexes. The workspace is evaluated by the number of points in the reachable space. The carrying capacity is evaluated by the average static stiffness of each point in workspace. And the motion stability is evaluated

by the average dexterity of each point in workspace. Note the indexes related to the workspace, carrying capacity, and motion stability as $\lambda_1$, $\lambda_2$ and $\lambda_3$, respectively, and they can be expressed as:

$$\begin{cases} \lambda_1 = N \\ \lambda_2 = \dfrac{\sum_{i=1}^{N} \max(eig([\mathbf{J}^{-1}]^{\mathrm{T}} \cdot \mathbf{k} \cdot \mathbf{J}^{-1}))}{N} \\ \lambda_3 = \dfrac{\sum_{i=1}^{N} \sqrt{\dfrac{\max(eig(\mathbf{J}^{\mathrm{T}} \cdot \mathbf{J}))}{\min(eig(\mathbf{J}^{\mathrm{T}} \cdot \mathbf{J}))}}}{N} \end{cases} \tag{8}$$

where $N$ is the number of points in the reachable space, $\mathbf{k}$ is the joint stiffness matrix of 4-UPU, $\mathbf{J}$ is the Jacobian matrix of 4-UPU.

The combination of the workspace, carrying capacity and motion stability is taken as the objective function. Taking the weighted sum of $\lambda_1$, $\lambda_2$ and $\lambda_3$, the objective function can be expressed as

$$F_1(x) = w_1\lambda_1 + w_2\lambda_2 + w_3\lambda_3 \tag{9}$$

where, $w_1$, $w_2$, and $w_3$ are the weighting factors, which can be adjusted to satisfy different requirements. Considering that the vibration amplitude of the platform will generally not exceed the workspace when the vehicle is running on the road, and the carrying capacity and the motion stability of the mechanism have a greater impact on the weight and reliability of the platform, set $w_2$ and $w_3$ larger than $w_1$. Based on comparison and analysis of the results of the objective function with several groups of weighting factors, $w_1$, $w_2$ and $w_3$ are selected as 0.2, 0.4, 0.4.

The dimension parameters of the 4-UPU parallel mechanism are taken as design variables. They are the side lengths of fixed base $R_1$, $R_2$, the side length of moving platform $d$, and the initial length of limbs $L$, as shown in Fig.3. The range of variables depends on the installation space in the vehicles. In this paper, they should be subject to

$$\begin{cases} 300 \le L_i \le 350 \\ 60 \le d \le 85 \\ 200 \le R_1 \le 250 \\ 150 \le R_2 \le 200 \end{cases} \tag{10}$$

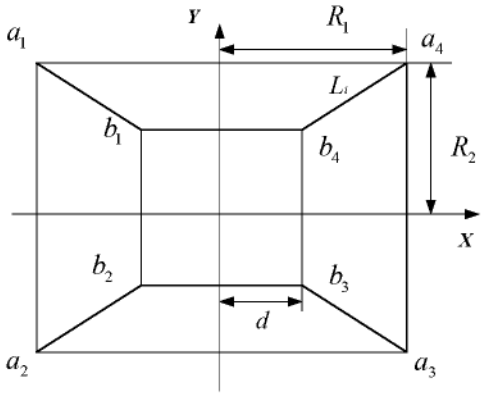


Fig.3 Declaration of the optimization parameters

The design variables are optimized by the sequential quadratic programming (SQP) method, and the optimization results are as follows: $R_1$=329, $R_2$=83.4, $d$=235.4, $L$=155.2. Substituting them into the kinematics model, the optimized workspace, carrying capacity and motion stability of the designed 4-UPU mechanism are obtained. The workspace plotted with Monte-Carlo method is shown in Fig.4(a). The performances of the carrying capacity and motion stability are expressed as the evaluation data of each point in workspace and represented by different colors, as shown in Fig.4(b). The smaller the value, the better the performance.

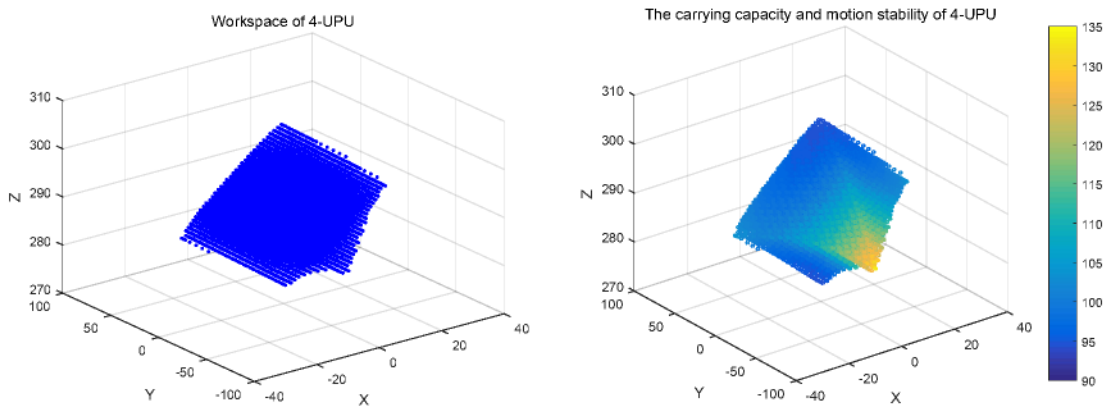


Fig.4 The optimized performance of 4-UPU (a) workspace (b) performance of the carrying capacity and motion stability

Projecting the center plane of evaluation data in workspace to the world coordinate system, the results are shown in Fig.5. The figures show that the workspace, carrying capacity and motion stability of 4-UPU are symmetrical in four vibration directions, which is helpful to improve the stability and controllability of the vibration isolation platform. The evaluation data in the central region is smaller than that in the peripheral region, which indicates that the mechanism has good adaptability to micro amplitude vibration.

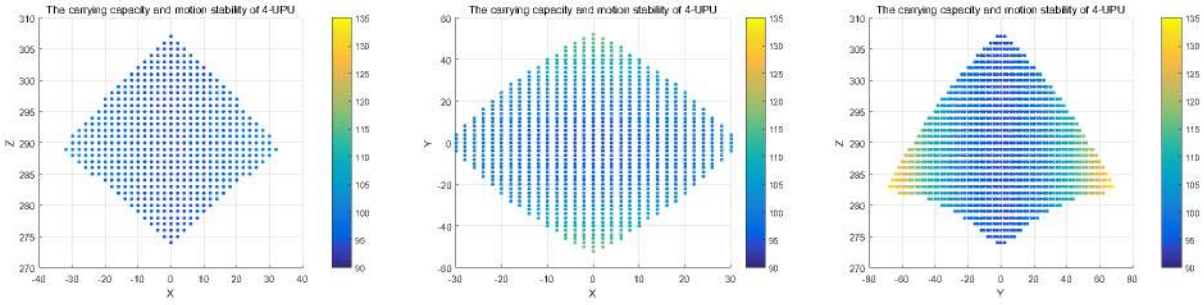


(a) (b) (c)

Fig.5 The projection of performance evaluation index (a) *XZ* plane (b) *XY* plane (c) *YZ* plane

## 3 Vibration response analysis

### 3.1 Stiffness matrix and damping matrix of MDVIP

Based on the obtained 4-UPU mechanism, replace the prismatic joints of the limbs of 4-UPU with the spring damper modules. Each module consists of a damper and two symmetrically arranged springs with guide rods to avoid overturning force and moments. The resulting vibration isolation platform is shown in Fig.6. To fulfill the requirements of axes, the universal joints are designed to connect with the platform through bearings and fix bolts, and connect with the spring damper module through fix blocks and connect blocks.

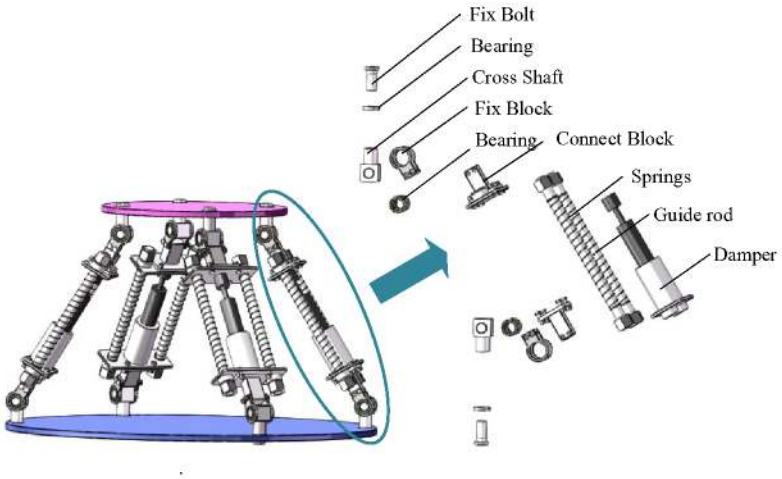


Fig.6 Scheme of the MDVIP

Assuming the forces and the torques exerted on the moving platform are concentrated in its center of mass, note the external forces on the moving platform as $\mathbf{f}=[f_x, f_y, f_z, T_z]^{\mathrm{T}}$, where, $f_x$, $f_x$, $f_x$ are the forces along *x*-, *y*- and *z*-axis, respectively, and $T_z$ is the torque around the *z*-axis.

Note the active force of limbs as $\boldsymbol{\tau}=[\tau_1, \tau_2, \tau_3, \tau_4]^{\mathrm{T}}$. Because the limbs are replaced by spring damper modules, the active forces caused by springs can be expressed as:

$$\boldsymbol{\tau} = \mathbf{k}\Delta\mathbf{s} \tag{11}$$

where, $\Delta\mathbf{s}$ is the virtual displacement of limbs, and $\Delta\mathbf{s}=[\Delta s_1, \Delta s_2, \Delta s_3, \Delta s_4]^T$. $\mathbf{k}$ is the stiffness matrix of springs, and $\mathbf{k}=diag(k_1, k_2, k_3, k_4)$. Where $k_i$ ($i$=1,2,3,4) is the spring stiffness of the $i$th limb.

Based on the virtual work principle and kinematics of parallel mechanism, the relationship between limbs and moving platform can be expressed as:

$$\begin{aligned} (\mathbf{k}\Delta\mathbf{s})^T\Delta\mathbf{s} &= \mathbf{f}^T\Delta\mathbf{e} \\ \Delta\mathbf{s} &= \mathbf{J}^{-1}\Delta\mathbf{e} \end{aligned} \tag{12}$$

where $\Delta\mathbf{e}$ is the virtual displacement of the moving platform.

From the equations above, the external force on the moving platform can be expressed as:

$$\mathbf{f} = \left([\mathbf{J}^{-1}]^T\mathbf{k}\mathbf{J}^{-1}\right)\Delta\mathbf{e} \tag{13}$$

Therefore, the stiffness matrix of the isolation platform can be expressed as:

$$\mathbf{K} = [\mathbf{J}^{-1}]^T\mathbf{k}\mathbf{J}^{-1} \tag{14}$$

Similarly, the damping matrix of the isolation platform can be expressed as:

$$\mathbf{C} = [\mathbf{J}^{-1}]^T\mathbf{c}\mathbf{J}^{-1} \tag{15}$$

where, $\mathbf{c}$ is the damping matrix of limbs, and $\mathbf{c}=diag(c_1, c_2, c_3, c_4)$. And $c_i$ ($i$=1,2,3,4) is the damping of the $i$th limb.

### 3.2 Damped vibration response

Based on the stiffness and damping matrix of the isolation platform, the vibration model of the platform is built as

$$\mathbf{M}\ddot{\mathbf{e}} + \mathbf{C}\dot{\mathbf{e}} + \mathbf{K}\mathbf{e} = \mathbf{F}(\mathbf{t}) \tag{16}$$

where, $\mathbf{e}$, $\dot{\mathbf{e}}$, $\ddot{\mathbf{e}}$ are the generalized displacement, velocity and acceleration vectors, respectively. $\mathbf{M}$ is the mass matrix of the platform and $\mathbf{F}(\mathbf{t})$ is the generalized force.

Assuming the external excitation exert on the MDVIP is mainly transmitted from the fixed base, the vibration model can be expressed as:

$$\mathbf{M}\ddot{\mathbf{e}} + \mathbf{C}\dot{\mathbf{e}} + \mathbf{K}\mathbf{e} = \mathbf{K}\mathbf{z}(\mathbf{t}) + \mathbf{C}\dot{\mathbf{z}}(\mathbf{t}) \tag{17}$$

To solve the vibration equations, the model ought to be decoupled. The eigenvectors $\mathbf{A}^{(n)}$ ($n$ =1, 2, 3, 4) of the undamped free vibration isolation platform are calculated and regularized as follows.

$$\boldsymbol{\varphi}^{(n)} = \frac{\mathbf{A}^{(n)}}{\sqrt{\mathbf{A}^{(n)\mathrm{T}}\mathbf{M}\mathbf{A}^{(n)}}} \quad (n=1,2,3,4) \tag{18}$$

where, $\varphi^{(n)}$ ($n$=1,2,3,4) is the regularized eigenvector.

Therefore, the regularization matrix is expressed as:

$$\boldsymbol{\Phi} = [\boldsymbol{\varphi}^{(1)}, \boldsymbol{\varphi}^{(2)}, \boldsymbol{\varphi}^{(3)}, \boldsymbol{\varphi}^{(4)}] = diag(\frac{1}{\sqrt{m}}, \frac{1}{\sqrt{m}}, \frac{1}{\sqrt{m}}, \frac{1}{\sqrt{I_z}}) \tag{19}$$

By multiplying the regularization matrix, the decoupled mass $\mathbf{M}'$, stiffness $\mathbf{K}'$ and damping matrix $\mathbf{C}'$ are expressed as follows.

$$\mathbf{M}' = \boldsymbol{\Phi}^{\mathrm{T}}\mathbf{M}\boldsymbol{\Phi} = \mathbf{I} \tag{20}$$

$$\mathbf{K}' = \boldsymbol{\Phi}^{\mathrm{T}}\mathbf{K}\boldsymbol{\Phi} = diag(\omega_1^2, \omega_2^2, \omega_3^2, \omega_4^2) \tag{21}$$

$$\mathbf{C}' = \boldsymbol{\Phi}^{T}\mathbf{C}\boldsymbol{\Phi} = diag(2\xi_1\omega_1, 2\xi_2\omega_2, 2\xi_3\omega_3, 2\xi_4\omega_4) \tag{22}$$

where, $\omega_r$ ($r$ =1, 2, 3, 4) is the natural frequency of damped vibration of the MDVIP, $\xi_r$ ($r$ =1, 2, 3, 4) is the damping ratio of the $r$-th vibration mode.

The decoupled vibration model is expressed as

$$\mathbf{M}'\ddot{\boldsymbol{\eta}} + \mathbf{C}'\dot{\boldsymbol{\eta}} + \mathbf{K}'\boldsymbol{\eta} = \mathbf{K}'\boldsymbol{\mu} + \mathbf{C}'\dot{\boldsymbol{\mu}} \tag{23}$$

where, $\boldsymbol{\eta}$, $\dot{\boldsymbol{\eta}}$, $\ddot{\boldsymbol{\eta}}$ are the decoupled generalized displacement, velocity and acceleration vectors, respectively, $\boldsymbol{\eta}$=[$\eta_1$, $\eta_2$, $\eta_3$, $\eta_4$]$^{\mathrm{T}}$, and $\boldsymbol{\mu}$, $\dot{\boldsymbol{\mu}}$ are the decoupled external excitation displacement and velocity vectors, $\boldsymbol{\mu}$=[$\mu_1$, $\mu_2$, $\mu_3$, $\mu_4$]$^{\mathrm{T}}$.

And the vibration equation in each vibration direction is decoupled into:

$$\ddot{\eta}_r + 2\xi_r\omega_r\dot{\eta}_r + \omega_r^2\eta_r = \omega_r^2\mu_r(t) + 2\xi_r\omega_r\dot{\mu}_r(t) \qquad (r=1,\ 2,\ 3,\ 4) \tag{24}$$

**3.3 Forced Vibration Response**

Based on the road roughness, the vibration transmitting to the vibration isolation platform can be decomposed into several simple harmonic vibrations with an amplitude no more than 5mm, and a frequency no less than 20Hz. Then the external excitation is assumed as simple harmonic vibrations:

$$\mu_r(t) = a_r\sin(\omega_{dr}t) \qquad (r=1,2,3,4) \tag{25}$$

where $\mu_r$ is the displacement of external excitation, $a_r$ is the amplitude and $\omega_{dr}$ is the natural frequency of external excitation.

And the vibration equations of parallel vibration isolation platform can be expressed as:

$$\ddot{\eta}_r + 2\xi_r\omega_r\dot{\eta}_r + \omega_r^2\eta_r = \omega_r^2 a_r \sin(\omega_{dr}t) + 2\xi_r\omega_r\omega_{dr}a_r\cos(\omega_{dr}t) \qquad (r = 1,\ 2,\ 3,\ 4) \tag{26}$$

Solving equation 26, one gets the vibration response of the MDVIP to harmonic excitation in four DOF directions:

$$e_r = B_r\sin(\omega_r t + \theta_r) \tag{27}$$

where $B_r$ is the amplitude and $\theta_r$ is the phase of the vibration response of the moving platform. And there are

$$B_r = a_r\sqrt{\frac{\omega_r^4 + (2\xi_r\omega_r\omega_{dr})^2}{(\omega_r^2 - \omega_{dr}^2)^2 + (2\xi_r\omega_r\omega_{dr})^2}} \tag{28}$$

$$\theta_r = \arctan\frac{2\xi_r\omega_r\omega_{dr}^3}{(\omega_r - \omega_{dr})^2 + (2\xi_r\omega_r\omega_{dr})^2} \tag{29}$$

And the vibration transmission rate $T$ of the isolation platform can be expressed as:

$$T = \frac{B_r}{a_r} = \sqrt{\frac{\omega_r^4 + (2\xi_r\omega_r\omega_{dr})^2}{(\omega_r^2 - \omega_{dr}^2)^2 + (2\xi_r\omega_r\omega_{dr})^2}} \tag{30}$$

It is noted that the smaller the vibration transmission rate $T$, the better the isolation performance of the MDVIP.



### 3.4 Optimization of the spring damper

To minimize the vibration transmission rate of MDVIP, the sum of vibration responses in the directions along *X*-, *Y*-, *Z*-axis and round *Z*-axis is taken as the objective function.

$$F_2(y) = \sum_{j=1}^{4} W_j f_j(y) \qquad (j = 1,2,3,4) \tag{31}$$

where, $f_j(y)$ is the vibration response amplitude in *j*th direction, and $f_j(y) = B_r$, $j$=$r$. $W_j$ is the corresponding weighting factor. Considering the vibration caused by road roughness is mainly concentrated on *X*, *Y*, *Z* directions, the relevant weighting factors, $W_1$, $W_2$ and $W_3$, are set greater than $W_4$ which is the weighting factor related to vibration response in the direction around *Z*-axis. Based on the comparison of the results with several groups of weighting factors, $W_1$, $W_2$, $W_3$, $W_4$ are selected as 0.3, 0.3, 0.3, 0.1, respectively. Vibration responses of isolation platform are related to the mass $m$ and moment of inertia $I_z$ of moving platform, as well as the spring stiffness $k_i$ and damping $c_i$ ($i$=1,2,3,4) of the $i$th limb. To keep the symmetry of MDVIP, the stiffness and damping parameters of each limb are set to be equal and let $k_1 = k_2 = k_3 = k_4 = k$, $c_1 = c_2 = c_3 = c_4 = c$. Take these parameters as the design variables, and note as:

$$\boldsymbol{y} = [m, I_z, k, c] \tag{32}$$

According to the design principle of vibration isolator, the constraint of damping ratio $\xi(=c/2\sqrt{mk})$ should be bigger than 0.03. Based on resonance theory, the natural frequency $\omega_r$ of the isolation platform should be smaller than $\sqrt{2}/2$ times of the minimum vibration isolation frequency, which is 20Hz. Then the optimization problem can be written as:

$$\begin{aligned} &\min F_2(m, I_z, k, c) \\ &s.t. \quad -\frac{c}{2\sqrt{mk}} + 0.03 \le 0 \\ &\omega_r - 10\sqrt{2} \le 0 \end{aligned} \tag{33}$$

The design variables are optimized by Genetic Algorithm, and the results are as follows: $m$=10.54, $I_z$=0.52, $k$=904.06, $c$=99.46.

Substituting the optimized parameters into the vibration model, the vibration responses of MDVIP with different amplitude and frequency in different vibration directions are shown in Fig.7. The red lines denote the vibration transmission rate $T$ with 5mm excitation amplitude.

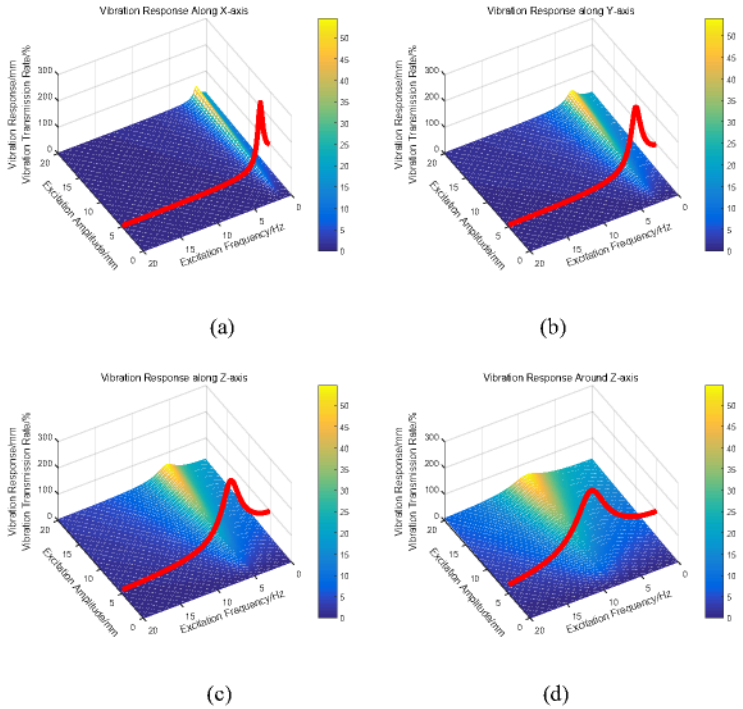


Fig.7 Vibration responses with different amplitude and frequency (a) Along $X$ (b) Along $Y$ (c) Along $Z$ (d) Around $Z$

It is observed from Fig.7 that with the increasing of the excitation amplitude, the vibration responses of the moving platform increase gradually and the resonance humps become wider and higher. Additionally, the vibration

response data show that the MDVIP can isolate the vibration with a frequency greater than 13.1 Hz, which makes it suitable for vibration isolation of sensitive devices in moving vehicles.

## 4 Vibration-isolation performance of the MDVIP

### 4.1 Numerical solution of the vibration response of the MDVIP

Exert a simple harmonic excitation with an amplitude of 5 mm and frequency of 20 Hz on the fixed base of the MDVIP in four directions respectively and calculate the vibration responses of the moving platform. The vibration response curves in four directions are shown in Fig.8 in the form of acceleration. The red solid lines and the blue dash lines denote the vibration response of the moving platform and the fixed base, respectively. The corresponding values of the vibration transmission rate $T$ in four DOF directions are shown in Table 2.

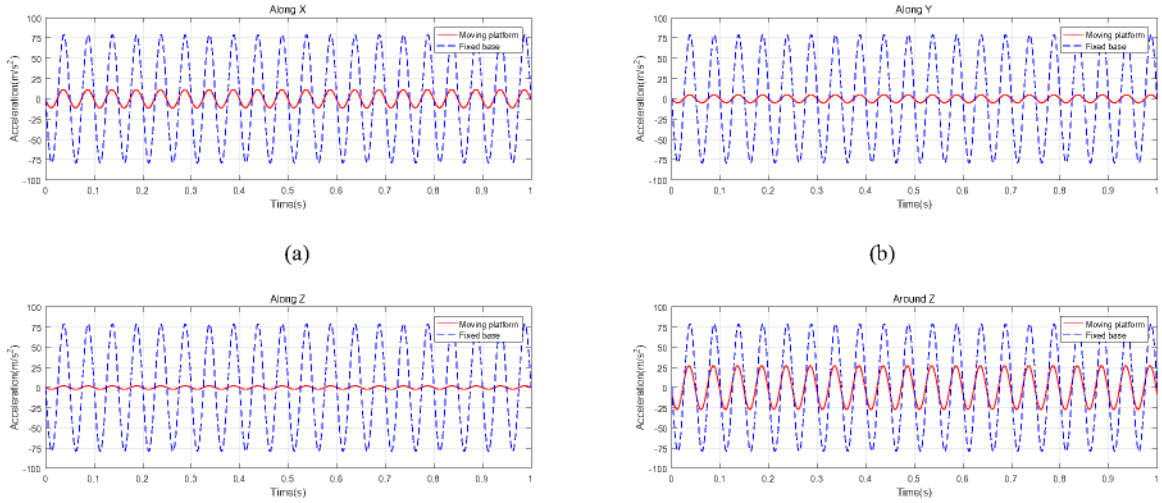


Fig.8 Numerical results of the vibration response of the MDVIP: (a) Vibration response along $X$-axis, (b) Vibration response along $Y$-axis, (c) Vibration response along $Z$-axis, (d) Vibration response around $Z$-axis

### 4.2 Simulation analysis of the MDVIP

As shown in Fig.9, the virtual prototype of the MDVIP is established and the same excitations are exerted on the fixed base in ADAMS to verify the correctness of the vibration model. The variation curves of the vibration response in each DOF direction are shown in Fig.10. The values of the vibration transmission rate $T$ in four DOF directions are listed in Table 2.

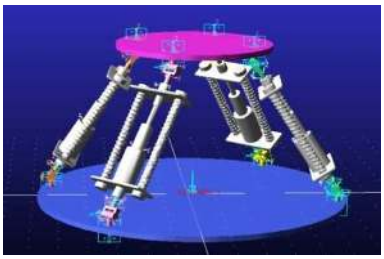

Fig.9 Simulation model of the MDVIP in Adams

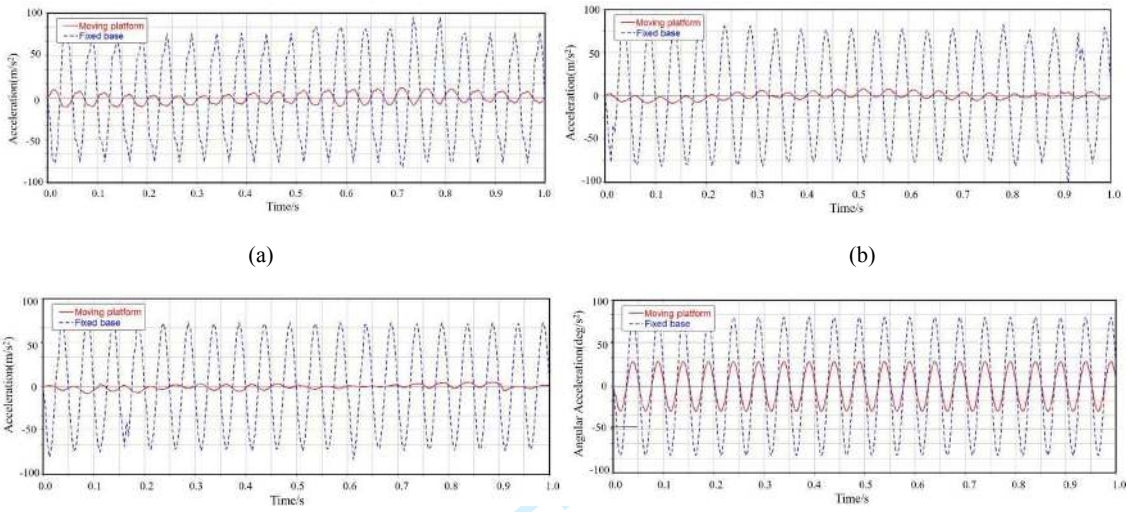


Fig.10 Simulation results of the vibration response of the MDVIP: (a) Vibration response along *X*-axis, (b) Vibration response along *Y*-axis, (c) Vibration response along *Z*-axis, (d) Vibration response around *Z*-axis

### 4.3 Experimental study of the MDVIP

The physical prototype is manufactured to carry out the experiments. The experiment system includes a vibration generation module, the MDVIP and an analysis module, as shown in Fig.11. In the vibration generation module, the disturbance signals are generated by a signal generator and converted to electrical signals by the amplifier. The electrical signals are transmitted to the exciter to produce vibration and the vibrations are exerted to the fixed base of the MDVIP. In the analysis module, the vibration signals of the fixed base and moving platform are collected by the accelerometers and stored by a data collector. By analyzing the vibration data in the host computer, the vibration isolation effect of MDVIP can be obtained. The devices and specifications involved in the experiment are listed in Table 1.

Table 1 Devices and specification

| Devices | Specification | | | | | |
|---|---|---|---|---|---|---|
| Signal generator | Type | | YE1311 | Frequency range/Hz | 2-2000 | |
| Amplifier | Type | | YE5872A | Current range/A | 3-13 | |
| Exciter | Type | | JZK-10 | Frequency range/Hz | 1-2000 | |
| | Maximum amplitude/mm | ± 10 | Maximum acceleration/g | 28 | Maximum output force/kg | 10 |
| MDVIP | Side length of Fixed Base $R_1$/mm | 329 | Side length of Fixed Base $R_2$/mm | 83.4 | Side length of Moving platform $d$/mm | 235.4 |
| | Initial length of Limbs $L$/mm | 155.2 | Mass of Devices $m$/kg | 10.54 | Inertia of Devices $I_z$/kg • m$^2$ | 0.52 |
| | Stiffness $k$/N/m | 904.06 | Damping $c$/N • s/m | 99.46 | | |
| Accelerometer | Type | CA-YD-186 | sensitivity/mV/g | 100 | Frequency range/Hz | 0.5-5000 |
| | operating temperature/℃ | -40-120 | Measuring error | 5% | Impact limit/g | 200 |
| | Measuring range/g | 50 | | | | |
| Data collector | Type | YE6231 | Number of channel | 4 | Error | ± 0.5% |

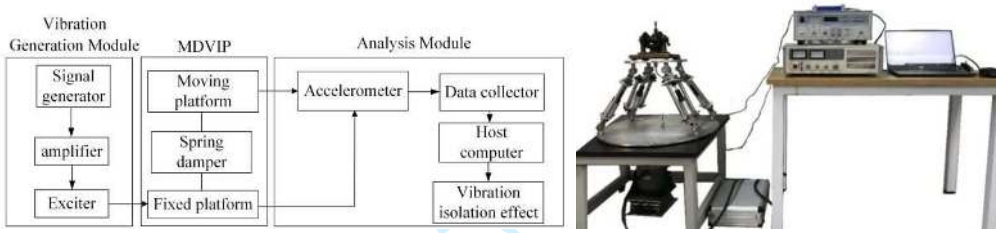


Fig.11 Experiment system of the MDVIP: (a) Scheme of the experiment system, (b) Prototype of the experiment system

Exert the simple harmonic excitations with an amplitude of 5 mm and frequency of 20 Hz on the fixed base of the MDVIP through the exciter in three axial directions, same as those used in numerical and simulation study. Collect the acceleration signals of the moving platform by the data collector and then process them in the host computer. The corresponding vibration responses in the above-mentioned directions are shown in Fig.12 in the form of acceleration. The vibration transmission rate $T$ is calculated by the RMS value of the vibration response of the moving platform and fixed base, and the results are shown in Table 2.

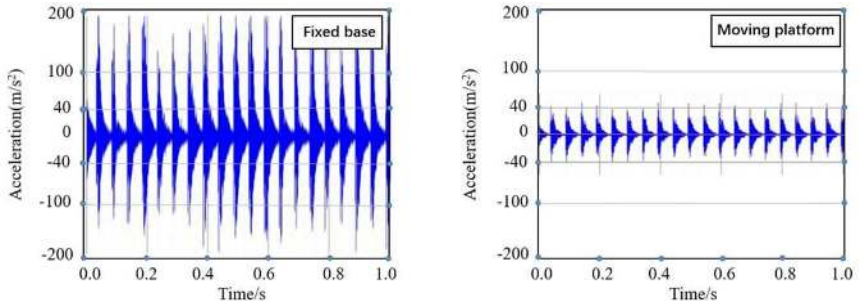


(a)

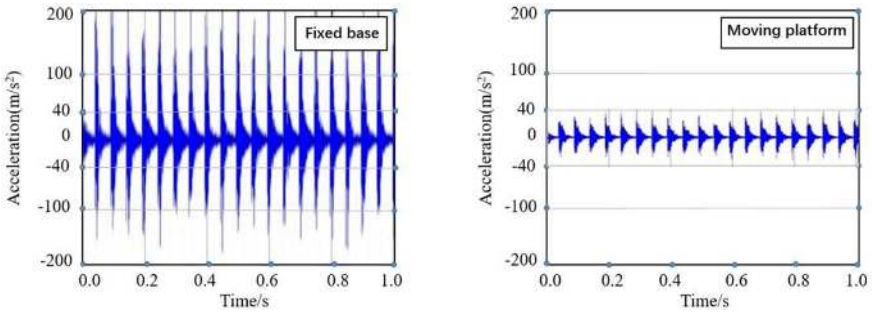


(b)

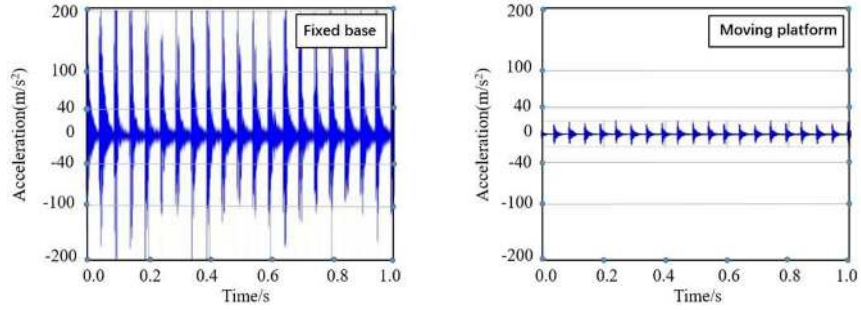


(c)

Fig.12 Experimental results of the vibration response to simple harmonic signals: (a) Vibration response along *X*-axis, (b) Vibration response along *Y*-axis, (c) Vibration response along *Z*-axis

Table 2 Comparison of the vibration-isolation performance in the concerned DOF directions

| Vibration transmission rate *T* | Along *X* | Along *Y* | Along *Z* | Around *Z* |
|---|---|---|---|---|
| Numerical value | 13.14% | 5.91% | 2.63% | 30.59% |
| Simulation value | 13.37% | 11.09% | 5.17% | 35.33% |
| Experimental value | 21.48% | 16.02% | 8.44% | -- |

From the results of calculation, simulation and experiments (shown in Fig.8, Fig.10 and Fig.12), it can be concluded that the vibration response amplitudes of the moving platform in each concerned direction have a significant reduction compared to the external excitation exerted on the fixed base. The data shown in table 2 demonstrates that the 4-UPU MDVIP can isolate at least 78.52% vibrations in the directions of *X*-, *Y*- and *Z*-axis and 64.67% in the direction around the *Z*-axis. The errors between calculation, simulation and experiments in four directions are less than 8%. The results show the correctness and effectiveness of the proposed solution.

## 5 Conclusion

In this paper, a novel 4-DOF multi-dimensional vibration isolation platform based on a 4-UPU low-mobility parallel mechanism is developed to isolate the vibration transferred from the running vehicles. The main works are as follows.

(1) The dimensional parameters of the 4-UPU parallel mechanism are designed through the optimization method by taking workspace, carrying capacity and motion stability into consideration.

(2) The dynamic model of the MDVIP based on a 4-UPU parallel mechanism is built to get the vibration response of the system and the parameters of the spring damper modules are optimized by Genetic Algorithm for better vibration isolation effect.

(3) The vibration isolation performance of the proposed MDVIP is verified by the numerical, simulation and experimental method. And the minimum vibration isolation rate of the MDVIP in the four concerned directions is no less than 64%.

(4) To reduce the errors between the results of experiments and numerical calculation, further efforts should be made to improve the theoretical model and the accuracy of manufacturing and assembly in the future.

**Acknowledgments**

This work was supported by National Natural Science Foundation of China (Grant No. 51175031) and Youth Program of National Natural Science Foundation of China (Grant No. 51505023).



**References**

Chi, W., Ma, S.J., Sun, J.Q. 2020. A hybrid multi-degree-of-freedom vibration isolation platform for spacecrafts by the linear active disturbance rejection control. Applied Mathematics and Mechanics, **4**: 1-14. https://doi.org/10.1007/s10483-020-2606-5.

Fan, X., Ma, J., Ji, R. 2018. Integrated Dynamic Modeling for a Stewart Platform. In Proceedings of the 37th Chinese Control Conference (CCC), Wuhan, China., 25-27 July 2018. IEEE, Wuhan, China. pp.1844-1848.

Geng, Z.J., Haynes, L.S. 1993. Six degree-of-freedom active vibration isolation using a Stewart platform mechanism. IEEE Transactions on Control Systems Technology, **10**(5): 725-744. https://doi.org/10.1002/rob.4620100510

Gu, J., Li, G.T., Li, B., et al. 2014. A ship active vibration isolation system based on a novel 5-DOF parallel mechanism. In Proceedings of 2014 IEEE International Conference on Information and Automation, Hailar, Hulun Buir, 28-30 July 2014. IEEE, Hailar, Hulun Buir. pp. 800-805.

Hauge, G.S., Campbell, M.E. 2004. Sensors and control of a space-based six-axis vibration isolation system. Journal of Sound and Vibration. **269**(3-5): 913-931. https://doi.org/10.1016/s0022-460x(03)00206-2.

Lee, D.O., Park, G., Han, J.H. 2016. Hybrid isolation of micro vibrations induced by reaction wheels. Journal of Sound and Vibration, **363**: 1-17. http://dx.doi.org/10.1016/j.jsv.2015.10.023

Li, B.B., Sun, T., Song, Y.M., et al. 2015. Stiffness analysis and experiment of a novel 5-DoF parallel kinematic machine considering gravitational effects. International Journal of Machine Tools and Manufacture, **95**: 82-96. https://doi.org/10.1016/j.ijmachtools.2015.04.012

Liu, L.K., Zheng, G.T., Huang W H. 2006. Octo-strut vibration isolation platform and its application to whole spacecraft vibration isolation. Journal of Sound and Vibration, **289**(4-5): 726-744. https://doi.org/10.1016/j.jsv.2005.02.040.

Liu, X. J., Han, G., Xie, F., et al. 2018. A novel acceleration capacity index based on motion/force transmissibility for high-speed parallel robots[J]. Mechanism and Machine Theory, **126**: 155-170. https://dx.doi.org/10.1016/j.mechmachtheory.2018.03.013

Pan, Y., Gao, F. 2017. Position model computational complexity of walking robot with different parallel leg mechanism topology patterns[J], Mechanism and Machine Theory, **107**: 324-337. http://dx.doi.org/10.1016/j.mechmachtheory.2016.09.016

Qin, C., Xu, Z., Xia, M., et al. 2020. Design and optimization of the micro-vibration isolation system for large space telescope. Journal of Sound and Vibration, **482**: 461-489. https://doi.org/10.1016/j.jsv.2020.115461

Selig, J.M., Ding, X. 2001. Theory of vibrations in Stewart platforms. In proceedings of 2001 IEEE/RSJ International Conference on Intelligent Robots and Systems, Maui, HI., 29 Oct.-3 Nov. 2001. IEEE, Maui, HI. pp. 2190-2195.

Song, Y.M., Lian, B., Sun, T., et al. 2014. A Novel Five-Degree-of-Freedom Parallel Manipulator and Its Kinematic Optimization. Journal of Mechanisms and Robotics, **6**(4): 1-9. https://doi.org/10.1115/1.4027742

Song. Y.M., Gao, H., Sun, T., et al. 2014. Kinematic analysis and optimal design of a novel 1T3R parallel manipulator with an articulated traveling plate. Robotics and Computer-Integrated Manufacturing, **30**(5): 508-516. http://dx.doi.org/10.1016/j.rcim.2014.03.006

Sun, T., Lian, B. 2018. Stiffness and mass optimization of parallel kinematic machine. Mechanism & Machine Theory, **120**: 73-88. https://doi.org/10.1016/j.mechmachtheory.2017.09.014

Sun, T., Song, Y.M., Li, Y., et al. 2010. Workspace Decomposition Based Dimensional Synthesis of a Novel Hybrid Reconfigurable Robot. Journal of Mechanisms and Robotics, **2**(3):191-220. https://doi.org/10.1115/1.4001781

Sun, T., Lian, B.B., Song, Y.M, et al. 2019. Elastodynamic optimization of a 5-DoF parallel kinematic machine considering parameter uncertainty. IEEE/ASME transactions on mechatronics, **24**(1): 315-325. https://doi.org/10.1109/TMECH.2019.2891355

Temmerman, J.D. Deprez,K., Anthonis, J., et al. 2004. Conceptual cab suspension system for a self-propelled agricultural machine, part 1: development of a linear mathematical model. Biosystems Engineering, **89**(4): 409-416. https://doi.org/10.1016/j.biosystemseng.2004.08.006.

Temmerman, J.D., Deprez, K., Anthonis, J., et al. 2005. Conceptual cab suspension system for a self-propelled agricultural machine, Part 2: operator comfort optimization. Biosystems Engineering, **90**(3): 271-278. https://doi.org/10.1016/j.biosystemseng.2004.08.007.

Thayer, D., Campbell, M., Vagners, J., et al. 2002. Six-axis vibration isolation system using soft actuators and multiple sensors. Journal of Spacecraft and Rockets, **39**(2): 206-212. https://doi.org/10.2514/2.3821.

Wang, M., Hu, Y,, Sun, Y., et al. 2020. An Adjustable Low-Frequency Vibration Isolation Stewart Platform Based On Electromagnetic Negative Stiffness. International Journal of Mechanical Sciences, **181**: 105-138. https://doi.org/10.1016/j.ijmecsci.2020.105714

Wang, Y., Miao, Z., Yin, X. 2017. Research on multi-dimensional vibration isolation control system based on a parallel mechanism. In Proceedings of the 14th IEEE International Conference on Information and Automation (ICIA), Macau SAR, China., 18-20 July 2017. IEEE, Macau SAR, China. pp.1115-1120.

Wei, J., Dai, J.S. 2019. Reconfiguration-aimed and Manifold-operation Based Type Synthesis of Metamorphic Parallel Mechanisms with Motion between 1R2T and 2R1T[J]. Mechanism and Machine Theory, **139**: 66-80. https://doi.org/10.1115/1.4044004

Wu, Y., Yu, K.P, Jiao, J., et al. 2015. Dynamic modeling and robust nonlinear control of a six-DOF active micro-vibration isolation manipulator with parameter uncertainties. Mechanism and Machine Theory, **92**: 407-435. https://doi.org/10.1016/j.mechmachtheory.2015.06.008.

Wu. Y., Yu, K., Jiao, J., et al. 2017. Dynamic isotropy design and analysis of a six-DOF active micro-vibration isolation manipulator on satellites. Robotics and Computer-Integrated Manufacturing, **49**: 408-425. https://doi.org/10.1016/j.rcim.2017.08.003.

Yang, F., Niu, J.C, Li, K.P., et al. 2013. Study on frequency tuning of parallel mechanism for reducing vibration. Applied Mechanics and Materials, **905**: 275-277. https://doi.org/10.4028/www.scientific.net/AMM.275-277.905.

Yang, X., Wu, H., Chen, B., et al. 2019. Dynamic modeling and decoupled control of a flexible Stewart platform for vibration isolation. Journal of Sound and Vibration, **439**: 398-412. https://doi.org/10.1016/j.jsv.2018.10.007

Yang, X., Wu, H., Li, Y., et al. 2020. Dynamics and Isotropic Control of Parallel Mechanisms for Vibration Isolation. IEEE/ASME Transactions on Mechatronics, **49**:408-425. http://dx.doi.org/10.1016/j.rcim.2017.08.003.

Ye, W., He, L., Li, Q. 2018. A New Family of Symmetrical 2T2R Parallel Mechanisms Without Parasitic Motion[J]. Journal of Mechanisms & Robotics, **10**(1):011006. https://doi.org/10.1115/1.4038527

Yi, T.D., Li, B., Wang, N. 2014. Analysis and optimization of a vibration isolation platform based on 6-DOF parallel mechanism. Key Engineering Materials, **625**: 748-753. https://doi.org/10.4028/www.scientific.net/KEM.625.748.

Zhou, J., Wang, K., Xu, D., et al. 2017. A Six Degrees-of-Freedom Vibration Isolation Platform Supported by a Hexapod of Quasi-Zero-Stiffness Struts. Journal of Vibration and Acoustics, **139**(3):502-507. https://doi.org/10.1115/1.4035715